

# Magnetic Pulse Acceleration

O. Gafri, A. Izhar, Y. Livshitz , V. Shribman

Pulsar Ltd., Yavne, Israel. P.O.B 421, Yavne, Israel

## Abstract

*The present work is dedicated to describing works in the spheres of simulation, calculation, and experimental results of acceleration by pulsed electromagnetic forces where strain rates of 10,000 - 50,000 s<sup>-1</sup> are common. The goal is to design a multidisciplinary model that will overcome the shortcomings of 'normal' simulation methods that solve the EM field and then apply the solution in a mechanical analysis. Improved numeric models for virtual simulation of magnetic pulse processes are detailed, along with the pulse-power equipment and a special measurement system developed to verify these models and to determine material property data. These measure both radial velocity and axial speed (collision-point progression) for tube forming and / or welding processes, while logging the pulse current and magnetic field. The results show good a correlation between test and multiphysics model and provide valuable new insights, as well as an extraction of critical parameters by way of a comparison between calculated and measured data for materials such as aluminum alloys, copper, and steel.*

## Keywords

Electromagnetic forming, Process modeling, Verification, High speed testing methods

## 1 Introduction

Magnetic-Pulse Forming and Welding (MPF, MPW) can be useful technologies for industrial fabrication with many benefits compared to conventional welding, stamping, hydroforming, explosive forming/welding, etc. [1-4]. To do that, however, one needs to tailor the velocity field of the flyer (accelerated part) which, in turn, depends both on the shifting magnetic field (time-dependent and variable due to magnetic-mechanical interaction and physical flyer displacement) and on the momentary geometry and properties of the flyer in-flight.

For magnetic pulse processes to enter into industrial use a method had to be derived by which a client's vision or existing application can be quickly and reliably transformed to an optimal MP process with all its major parameters (and parameter tolerance effect) calculated and the proper electrical and physical design recommended. Virtual process modeling is the

best way to view and analyze the process in action, as the short process duration (2 – 20  $\mu$ sec) and the nature of the system and process combine to make photography very hard (the part is enclosed and obscured by the coil, die, etc., moves at some 100's m/s, deforms at several km/s, and produces flashes that drown out the picture).

'Normal' methods, such as solving the EM field and then applying the sum body forces as 'pressure' in a mechanical Finite-Element Analysis (FEA), either directly (as pressure-time function in a transient analysis) or using an iterative EM/MEC step (with or without adaptive re-meshing), had several shortcomings, such as difficulty to model an inter-related phenomenon and taking several hours for entering the model geometry, and sometimes days for solving the loosely-coupled magneto-mechanical cycles.

## 2 Multi-physical model

### 2.1 Magnetic pulse equipment

The system to be modeled has a Capacitive Pulse-Current-Generator (PCG), connections for pulse currents (terminals, pulse cables, bus-bars, etc.), an optional Current-Augmenting pulse Transformer (CAT)[4,5], a load composed of a flat or cylindrical Coil of 1 or more windings or plates, i.e. Work Coil (WC)[1,2], an optional Flux-Concentrator or Field-Shaper (FS)[2,3], and 1 or more parts inserted in the "business end", i.e. Work-Pieces (WP<sub>#</sub>), having a tubular or flat geometry. All these items (except WP) were made in-house and their R/C/L values and  $K_{B:l}$  magnetic transference ratio (i.e. magnetic field level and shape for a given driving current) were tested, measured, and entered into a database[4]. Table 1 lists the Pulsar PCG's and their properties.

| Energy [kJ] | Rated volts | Rated pulse A | Self R <sub>o</sub> | Self L <sub>o</sub> | Self C <sub>o</sub> | Own S.C. frequency | PCG (e=prototype) |
|-------------|-------------|---------------|---------------------|---------------------|---------------------|--------------------|-------------------|
| 5           | 10,000      | 100 kA        | 6.70                | 100.0               | 100 $\mu$ F         | 50.05 kHz          | MP5-10-e          |
| 7           | 8,725       | 200 kA        | 9.50                | 82.00               | 184 $\mu$ F         | 39.92 kHz          | MP7-9             |
| 10          | 10,000      | 400 kA        | 20.0                | 79.25               | 200 $\mu$ F         | 34.57 kHz          | MP10-10-e         |
| 12          | 24,500      | 400 kA        | 7.20                | 44.19               | 40 $\mu$ F          | 119.00             | MP12-25           |
| 20          | 25,000      | 800 kA        | 26.0                | 26.80               | 80 $\mu$ F          | 76.51 kHz          | MP20-25-e         |
| 20          | 9,000       | 800 kA        | 1.80                | 29.97               | 552 $\mu$ F         | 38.84 kHz          | MP20-9            |
| 25          | 25,000      | 400 kA        | 4.23                | 46.09               | 80 $\mu$ F          | 82.56 kHz          | MP25-25           |
| 25          | 8,515       | 1000 kA       | 1.52                | 26.39               | 690 $\mu$ F         | 37.02 kHz          | MP25-9            |
| 30          | 6,000       | 250 kA        | 3.00                | 120.0               | 1.7 mF              | 10.96 kHz          | MP30-6-e          |
| 40          | 9,000       | 800 kA        | 8.50                | 39.07               | 1.1 mF              | 16.96 kHz          | MP40-9-           |
| 100         | 25,000      | 1600 kA       | 1.41                | 16.46               | 320 $\mu$ F         | 69.00 kHz          | MP100-25          |

**Table 1: Properties of Commercial Pulse Generators**

## 2.2 Modeling

Work was initially carried out using commercial finite-element software (various EM+ME FEA), but the high cost, long solving time, and difficulties in modeling some inter-linked phenomena soon led to the development of a proprietary MP-code. For the issue of tailoring the optimal process for a given application (i.e. optimal magnetic waveform to achieve required impact conditions with minimum charge energy, minimum component heat-up, and no over-stressing of components) two main approaches were used:

### 2.2.1 Energy-time iteration

In this method, the pulse is calculated as the system step response from the initial energy charge with momentary voltage/current/field strength values re-calculated at each time-step based on remaining electric energy and the new system geometry (as the workpiece, coil and FS deform due to magnetic forces). The geometry for the next time-step is then calculated based on magnetic “pressure”, kinetic energy, and mechanical deformation forces.

### 2.2.2 Force-translation iteration

This method assumes the magnetic field intensity to act as a simple decaying sine wave and calculates the body forces caused by magnetic repulsion and induction heat. Part acceleration under those forces is calculated, yielding the radial velocity profile along the part.

Both above systems base their calculations on a [client-specified] given geometry and material properties and the database of pulse current generators, coils, and field shapers.

These fast-solving programs sort through the possible combinations, find feasible combinations (those that yield the required impact velocity and angle without exceeding the allowed charge voltage, peak current, coil stress, etc.), sort for the optimum combination (minimum energy), and issue a list of the best combination for sample production.

The same models can then explore the effect of modifying the process parameters (MPF capacitance, coil length, number of winds, workpiece length inside field-shaper, and modification of workpiece diameter or thickness) to issue a list of recommendations as to how to build a suitable commercial system.

## 2.3 Test design

2 known MPW processes, for which waveforms for current and magnetic field were already measured in the methods listed below, were selected as a test case. The force-time model (fastest) was repeatedly run with changing parameters  $K_{EFS}$ , then  $\{R,L\}_e$ , then  $\sigma_d$ , until the calculated current waveform and magnetic waveform matched exactly to the test waveforms. The extracted  $K_{EFS}$ ,  $\{R,L\}_e$ , and  $\sigma_d$  parameters were used for the force-translation model and for an FEA model that served as control group.

The results from both models were similar to those obtained by FEA (figure 5) and solving took only a few minutes, compared to over 3 hours it took the FEA (50x8 elements grid, 64 contact elements, 2-D cylindrical, 2500 time-steps, 1.33MHz IBM PC). The results from both the velocity-versus-time profiles from the commercial FEA and the new algorithms were then compared to those recorded during the actual tests, verifying correctness.

### 2.3.1 Magnetic pulse equipment

The two processes selected for this test to cover a wide spectrum are listed under Figure 1.

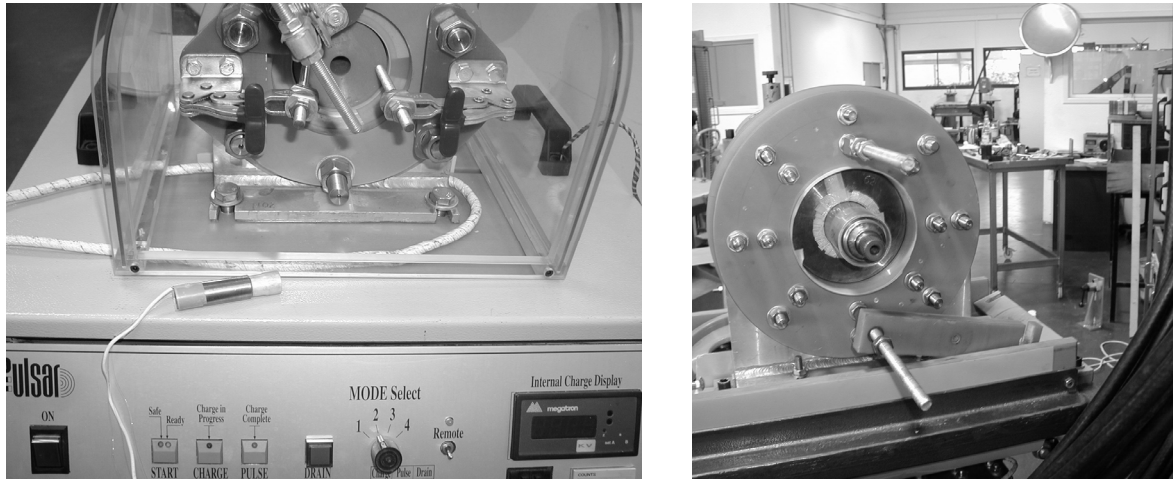


**Figure 1.** Test samples.

*Left: 1mm Al 1000 12.5mm diameter welded to 10mm steel using 2.8kJ on a 5kJ PCG. 6 plate x300° Bitter coil and D=72;X=75 by d=15;z=12 Bronze FS. ~13 TI*

*Right: 2mm Al 6061-T4 32mm diameter welded to 23mm steel using 40kJ on a 100kJ PCG, 3x270° plate Bitter coil and D=105;X=102 by d=35;z=22 FS. ~32 TI*

### 2.3.2 High-Speed measurement system

To verify the model prediction, measurements were taken of all critical process parameters. Coil current was measured using a “Rogowsky” pickup coil w. RC integrator. Magnetic field and distribution in the work-zone were measured by a thin axial probe (0.2mm thick x 5 or 20 mm wide with one or more 2mm sensor zones, placed between FS and driven part). The system for measuring radial “implosion” velocity is shown below (Figure 2).

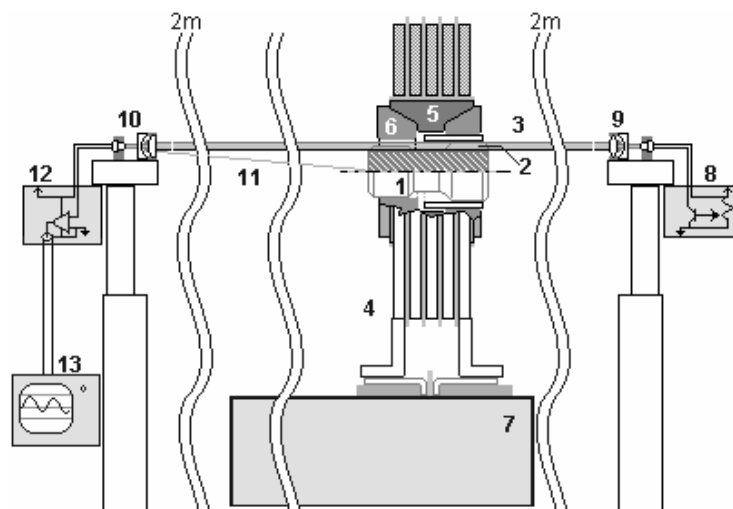


**Figure 2:** Laser velocimeter for  $V_r$

*1) inner workpiece. 2) light slot, the height of the acceleration gap, w. laser through-beam 1mm wide (a partial shadow “dead-zone” occurs near the edge of the driven workpiece #3)*

4) work coil 5) flux concentrator/FS 6) insulating part-positioning caps 7) pulse current generator. 8) laser power supply 9) collimator / line-generator optics 10) laser target 11) reflected centering beam 12) 50MHz analog optical sensor 13) data acquisition.

This system measures the % remaining beam power as the beam is being eclipsed by the workpiece imploding, then transforms the beam power record to gap height record, using a pre-calibrated gap:power transfer function to calculate  $dr/dt$ , i.e.  $V_r(t)$ , of the fastest point. To measure the contact progression velocity  $V_c$ , a system composed of a flexible adhesive sensor is attached over the inner workpiece, as shown below (Figure 3):

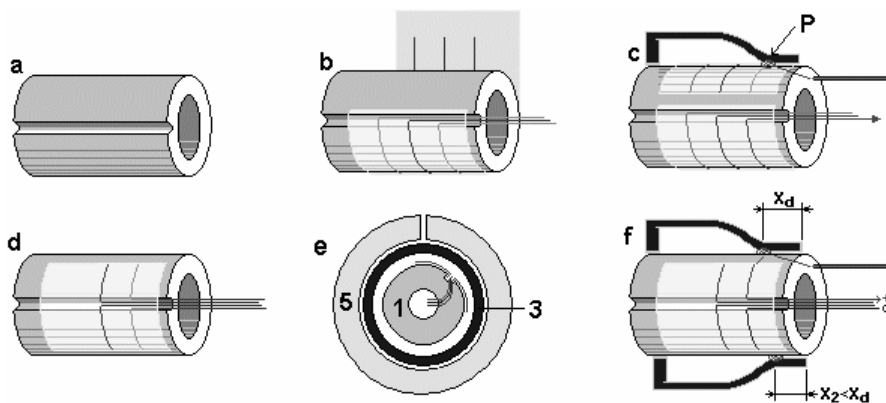


**Figure 3:** Axial velocity probe

- a) Inner workpiece with stepped groove.
- b) Flexible wrapping with varnish-coated filaments at set intervals (this sensing "Comb" of 360° coverage measures  $\text{Max}(V_c)$  )
- c) During pulse process, as contact point [P] pass over each electrode, the pinch flattens the filament to crack the insulating coat and shorts the output to ground. Steps in the groove can serve to cut the shorted sense section as P moves further so that each channel generates several on-off signals.
- d) Another variant with left-right 90° coverage, used to measure the effect of field-shaper gap on field uniformity:
  - e) When placed in the shaper so that one "Comb" is under the gap-affected zone, the offset in signals can be measured:
  - f) Due to the drop in field intensity near the gap  $V_c$  is lower and contact will only reach position  $X_2$  at the time the unaffected side reach  $X_d > X_2$ .

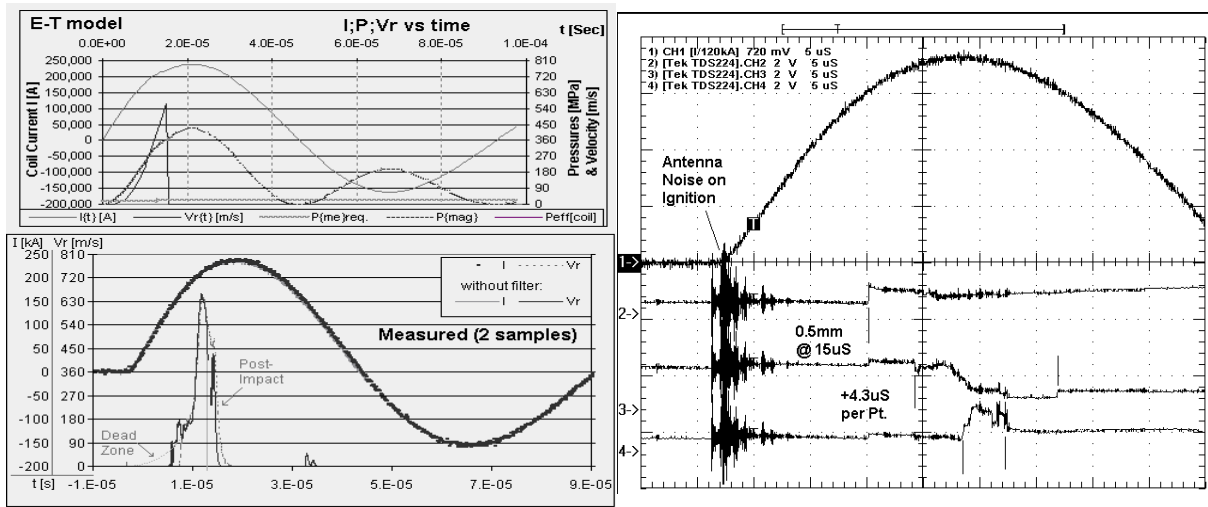


**Figure 4:** Model results vs. actual I:Vr measured at test and contact point progression from Vc-meter (Current delayed 3.2uS due to acquisition) showing Vc=4mm/4.3uS =930m/S for test geometry #2 (higher impact angle)

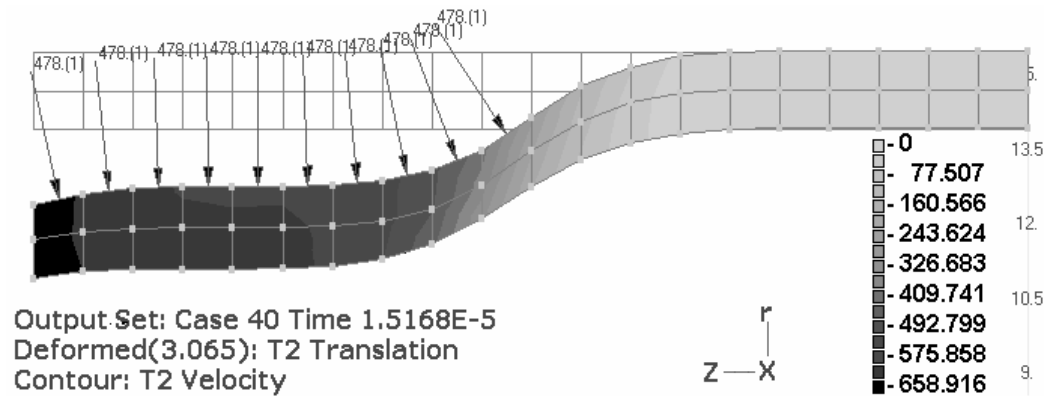


**Figure 5:** Model verified using conventional Finite-Element Analysis (screen shot Curtsy MSC NASTRAN)

### 3 Additional insights from the multi-physics model

The inclusion of electric-magnetic-thermal-mechanical to a unified model, stated as sparse-matrix solution with enough computational power to model the entire system, has resulted in some useful new insights into the physical behavior of the MP process itself, such as the compression of the current skin-layer due to  $dL/dt$  shift from mechanical deformation, which was later verified by testing, and has major effects on coil / FS design and lifetime [2].

## 4 Conclusions

For an industry-oriented company, with R&D focusing on improving the efficiency, stability, and durability of pulse-power systems for high magnetic field generation, commercial FEA is best replaced by faster and more physically-accurate computer models.

Researchers in the sphere of EM pulses (and EM forming in particular) can also benefit from employing a multi-physics model with total-system simulation capacity, as these models also give the magnetic, thermal, and stress profile of other major components (the coil, FS, etc.) and can prove to be valuable for designing these parts to withstand repetitive pulses.

Models for simulating and optimizing the electro-magnetic-mechanical coupled process of magnetic pulse acceleration should take into account physical dimensions, electrical and mechanical properties of all materials comprising the system (coil, field shaper, accelerated part, driven part, and impacted part.) The models serve for optimizing the pulse current generator (PCG) design, inductor's system parameters, and the pulse regime itself for any given (industrial) applications.

This paper shows that a low-cost measuring system can be employed for capturing the electrical and mechanical behavior of the electro-magnetic forming process and the model output matched the actual behavior by setting the correct factors (one main benefit of the measurement methods is that it enables the "fine-tuning" of the mathematical models by assembling a database of otherwise unknown parameters, such as material properties at ultra-high deformation rates, exact field distribution ( $X_{(x)}$ ) in FS work-zone, welding conditions for specific bimetallic combination, etc.) This data is automatically generated by converging to the parameters that "force" the model prediction to fit with actual test data.

Electromagnetic and mechanical phenomena regarding the behavior of Field Shapers (FS) and trapezoidal mono-wind coils during core collapse were noted and identified, leading to new improved designs. So far, coils and flux concentrators of 10-30TI (100-300 kGauss) have been designed to withstand several 10,000s pulses at 4PPM repetitive operation, powered by compact pulse current generators with capacitor energy storage (5-100kJ) and 1kA-1.5MA output (or more, using MA-level pulse transformers).

## References

- [1] *Livshiz, Y; Gafri, O.:* Technology & equipment for industrial use of pulse magnetic fields. Proceedings of 12<sup>th</sup> IPPC, Monterey, CA, 1999, p. 475-478.
- [2] *Livshiz, Y; Izhar, A.; Gafri, O.:* One turn coil for industrial use of magnetic pulse processes. Proceedings of 9<sup>th</sup> Mega-Gauss Conference, 2002, p. 125-131.
- [3] *Livshiz, Y; Izhar, A.; Gafri, O.:* One-turn coil and field-shaper design for industrial use of pulse-power magnetic processes. Proceedings of 14<sup>th</sup> PPC, 2003, #10397.
- [4] *Izhar, A.; Livshitz, Y.:* Adapting Pulse-Power generators to commercial and laboratory applications. Proceedings of IEE pulsed power seminar, Loughborough UK, 2003. #11.
- [5] *Izhar, A.; Livshitz, Y.:* High-voltage / high-current pulse power for civil, commercial, research & military test applications –Part III– Multi-Mega-Ampere pulse transformers, Proceedings of 15<sup>th</sup> IEEE Pulse Power Conference, 2005, #10172.